Electronic Supplementary Material (ESI) for Sustainable Energy & Fuels.

Supplementary Information

Iron-Doped Cobalt Phosphate 1D Amorphous Ultrathin Nanowires as Highly Efficient Electrocatalyst for Water Oxidation

Jifu Zhang, [a] Xueling Tan, [a] Wei Wang,[a,b] Lixin Cao, *[a] and Bohua Dong *[a]

[a] School of Materials Science and Engineering, Ocean University of China, 238 Songling Road, Qingdao, 266100 P. R. China.

[b] Aramco Research Center Boston, Aramco Services Company, Cambridge, MA02139, USA.

* Corresponding authors' Emails: dongbohua@ouc.edu.cn (B. Dong) and caolixin@ouc.edu.cn (L. Cao)

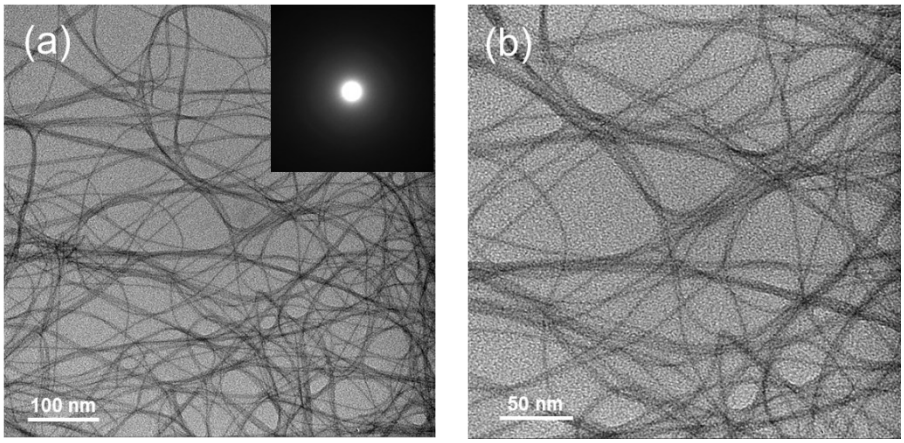

Fig. S1 TEM images of Am $Co_3(PO_4)_2$ nanowires. The inset of (a) is the corresponding SAED pattern.

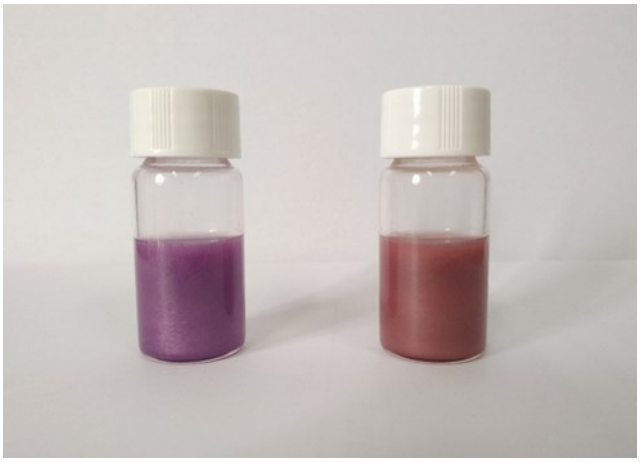

Fig. S2 Photograph of cyclohexane dispersion of Am $Co_3(PO_4)_2$ nanowires (left) and Am Fe-$Co_3(PO_4)_2$ ultrathin nanowires (right).

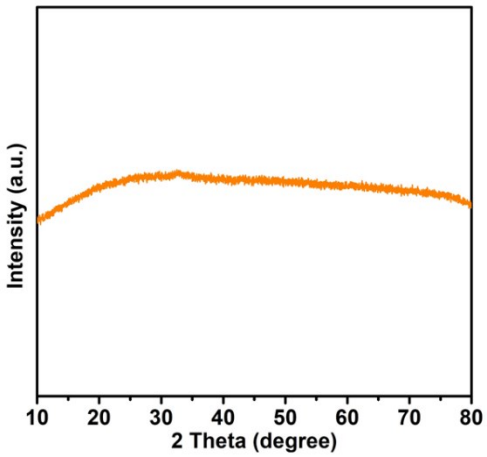

Fig. S3 The XRD pattern of Am Fe-$Co_3(PO_4)_2$ ultrathin nanowires.

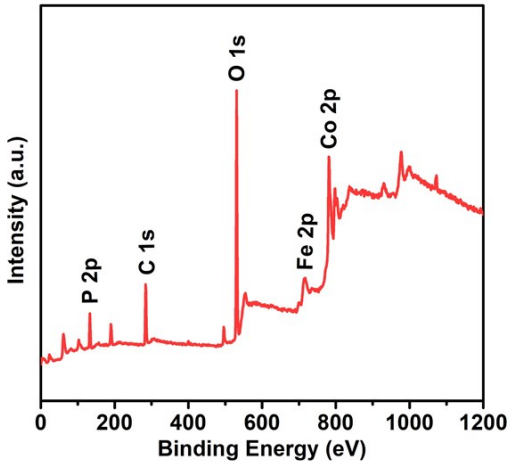

Fig. S4 XPS survey spectrum of Am Fe-$Co_3(PO_4)_2$ ultrathin nanowires.

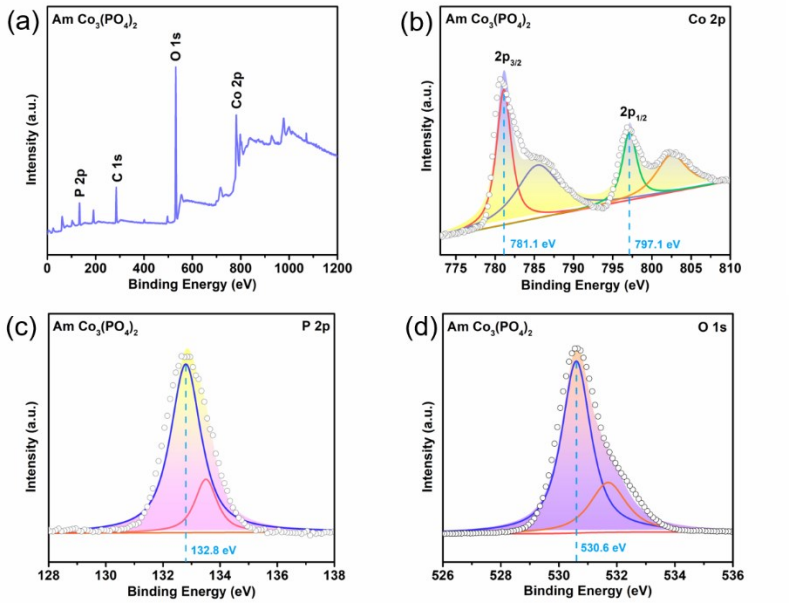

Fig. S5 (a) XPS survey spectrum, (b) Co 2p XPS spectrum, (c) P 2p XPS spectrum and (d) O 1s XPS spectrum of Am $Co_3(PO_4)_2$.

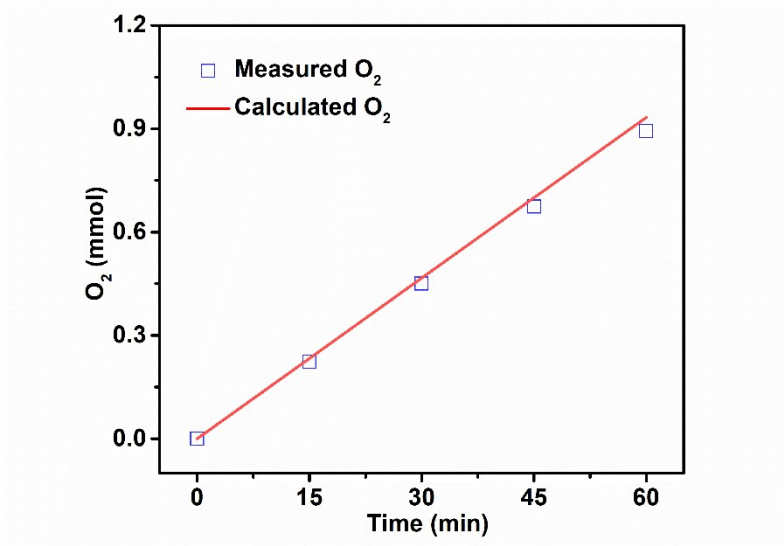

Fig. S6 The amount of theoretically calculated and experimentally measured oxygen as a function of time for Am Fe-$Co_3(PO_4)_2$ at a constant current density of 100 mA cm^{-2}.

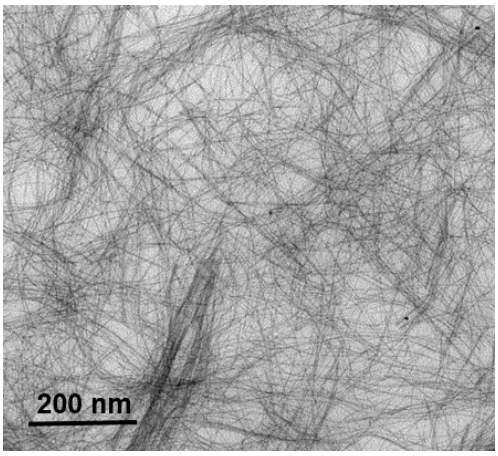

Fig. S7 TEM image of Am Fe-$Co_3(PO_4)_2$ ultrathin nanowires after stability test for the OER.

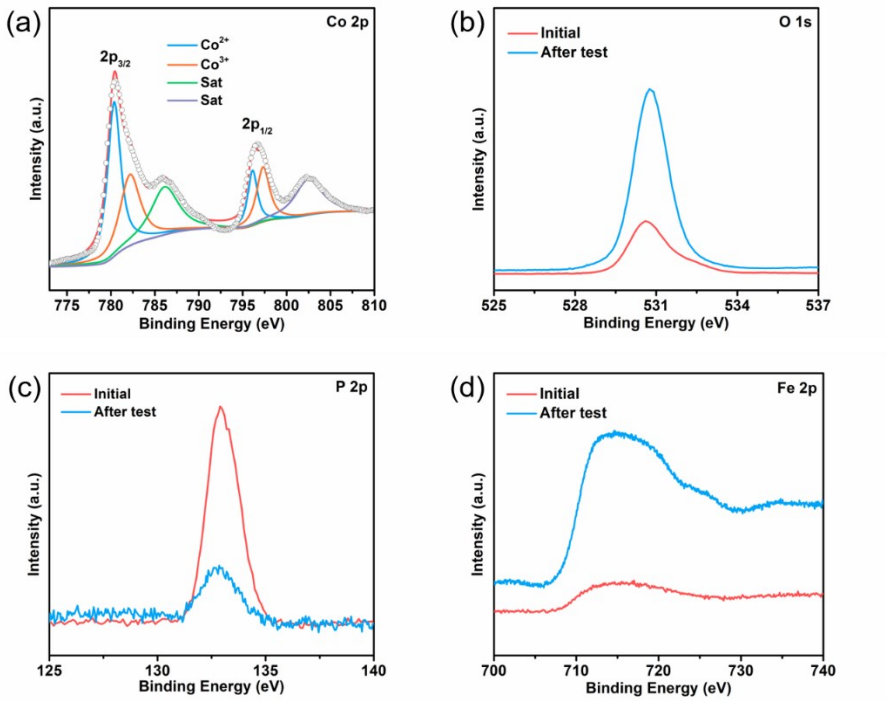

Fig. S8 XPS spectra of (a) Co 2p, (b) O 1s, (c) P 2p and (d) Fe 2p of Am Fe-$Co_3(PO_4)_2$ ultrathin nanowires after stability test.

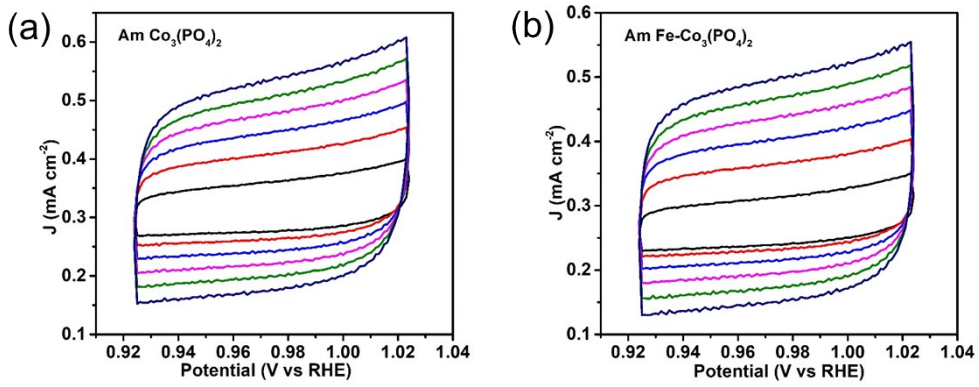

Fig. S9 Cyclic voltammograms of (a) Am $Co_3(PO_4)_2$ and (b) Am Fe-$Co_3(PO_4)_2$ with a potential window from 0.924 to 1.024 V at different scan rates in 1.0 M KOH.

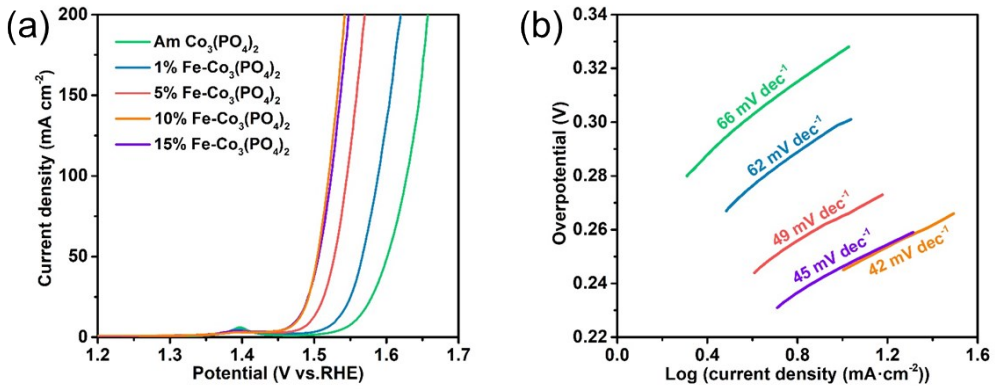

Fig. S10 (a) LSV curves of Am $Co_3(PO_4)_2$ and Am Fe-$Co_3(PO_4)_2$ with different amounts of Fe in 1.0 M KOH with 90% iR compensation. (b) Tafel plot for different catalysts derived from (a).

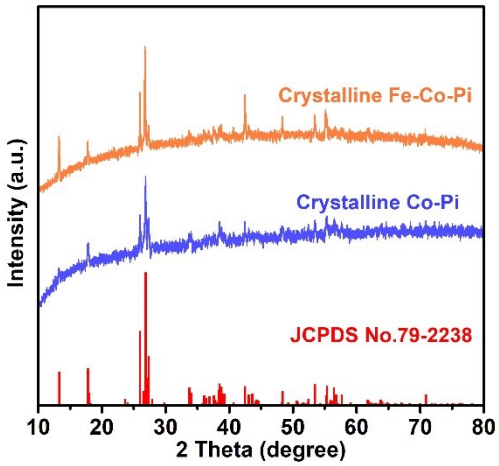

Fig. S11 XRD patterns of crystalline Co-Pi and crystalline Fe-Co-Pi.

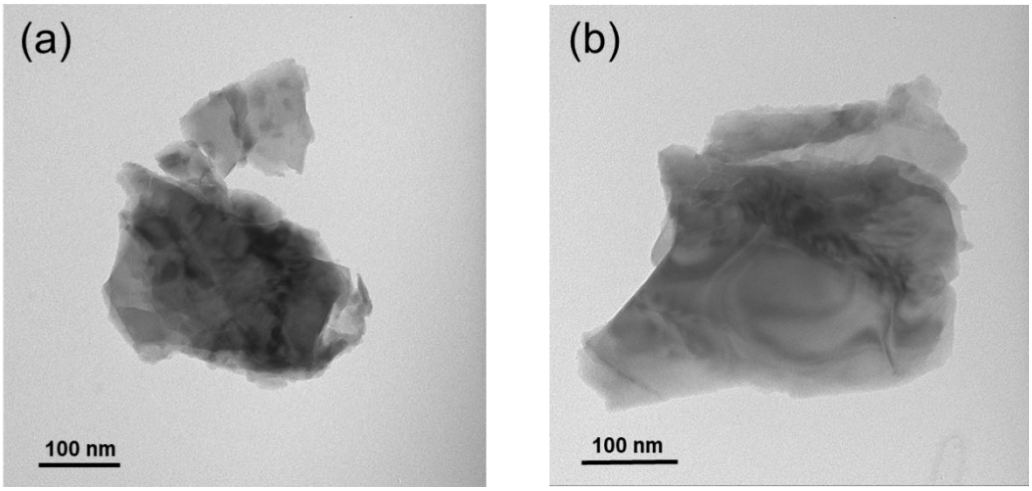

Fig. S12 TEM images of (a) crystalline Co-Pi and (b) crystalline Fe-Co-Pi.

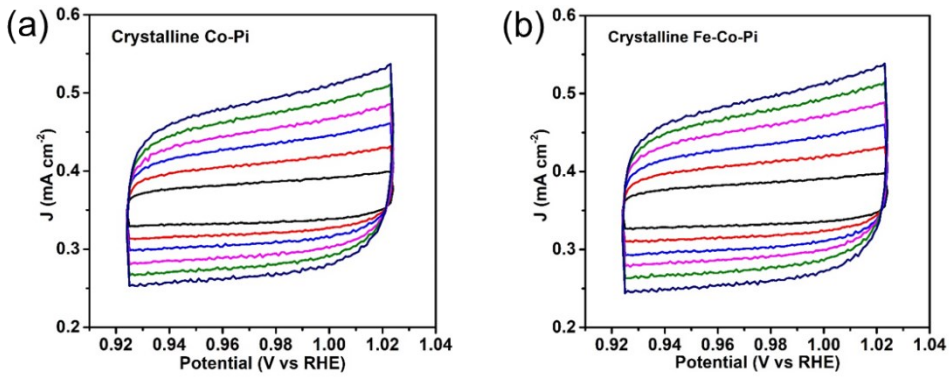

Fig. S13 Cyclic voltammograms of (a) crystalline Co-Pi and (b) crystalline Fe-Co-Pi with a potential window from 0.924 to 1.024 V at different scan rates in 1.0 M KOH.

Table S1. ICP-OES characterization of the Am Fe-$Co_3(PO_4)_2$ and crystalline Fe-Co-Pi samples.

Sample	Element	CC (mg kg^{-1})	Sample	Element	CC (mg kg^{-1})
Am Fe-$Co_3(PO_4)_2$	Fe	14631	Crystalline Fe-Co-Pi	Fe	27979
	Co	146165		Co	288568
Experimental atomic ratio of Fe:Co = 1:9.47			Experimental atomic ratio of Fe:Co = 1:9.77		

Table S2. Comparison of OER performances for Am Fe-$Co_3(PO_4)_2$ ultrathin nanowires with previously reported electrocatalysts in the alkaline media.

Catalysts	Electrolyte	Η@j=10 mA cm^{-2} (mV)	Tafel slope (mV dec^{-1})	Reference
Am Fe-$Co_3(PO_4)_2$	1 M KOH	245	42	This work
CoFeZr oxides/NF	1 M KOH	248	54.2	Adv. Mater. 2019, 1901439
FeOOH(Se)/IF	1 M KOH	287	54	J. Am. Chem. Soc. 2019, 141, 7005-7013
a-NiFeMo oxides	0.1 M KOH	280	49	Angew. Chem. Int. Ed. 2019, 58, 15772 –15777
Ar-NiCoP|V	1 M KOH	246	70.4	J. Mater. Chem. A, 2019, 7, 24486
$Co_3(OH)_2(HPO_4)_2$/NF	1 M KOH	240	69	Adv. Funct. Mater. 2019, 29, 1808632
CoFe-MOF-OH NF	1 M KOH	265	44	ACS Catal. 2019, 9, 7356−7364
NiCoFe@NiCoFeO NTAs/CFC	1 M KOH	201	39	J. Am. Chem. Soc. 2019, 141, 8136−8145
Mo-CoOOH	1 M KOH	305	56	Nano Energy 48 (2018) 73–80
Fe–Co–2.3Ni–B	1 M KOH	274	38	Adv. Energy Mater. 2018, 8, 1701475
Fe-$NiSe_2$ UNWs	0.1 M KOH	268	41	Angew. Chem. Int. Ed. 2018, 57, 4020–4024
CoPPi nanowires	1 M KOH	359	54.1	Small 2018, 14, 1801068
CoFe-H nanosheets	1 M KOH	280	28	Adv. Funct. Mater. 2017, 27, 1603904
Fe-CoP/Ti	1 M KOH	230	67	Adv. Mater. 2017, 29, 1602441
Ni:Pi-Fe/NF	1 M KOH	220	37	Chem. Mater. 2016, 28, 5659−5666
$Co_3(PO_4)_2$@N-C	1 M KOH	317	62	J. Mater. Chem. A, 2016,4, 8155